An effective-field theory study of hexagonal Ising nanowire: Thermal and magnetic properties

Yusuf Kocakaplan[a)] and Ersin Kantar[b)†]

[a)] *Institute of Science, Erciyes University, 38039 Kayseri, Turkey*
[b)] *Department of Physics, Erciyes University, 38039 Kayseri, Turkey*

(Received 31 July 2013; revised manuscript received 4 October 2013; published online 10 February 2014)

By means of the effective-field theory (EFT) with correlations, the thermodynamic and magnetic quantities (such as magnetization, susceptibility, internal energy, specific heat, free energy, hysteresis curves, and compensation behaviors) of the spin-1/2 hexagonal Ising nanowire (HIN) system with core/shell structure have been presented. The hysteresis curves are obtained for different values of the system parameters, in both ferromagnetic and antiferromagnetic cases. It has been shown that the system only undergoes a second-order phase transition. Moreover, from the thermal variations of the total magnetization, the five compensation types can be found under certain conditions, namely the Q-, R-, S-, P-, and N-types.

Keywords: hexagonal Ising nanowire, effective-field theory, hysteresis curve, compensation behavior

PACS: 68.35.Rh, 05.50.+q, 75.60.−d, 62.23.Hj **DOI:** 10.1088/1674-1056/23/4/046801

1. Introduction

In recent years, magnetic nanomaterials (such as nanoparticles, nanodots, nanofilms, nanorods, nanobelts, nanowires, and nanotubes) have attracted a great deal of interest, both theoretically and experimentally (see Refs. [1]–[6] and references therein). The reason is that these materials have many typical, peculiar, and unexpected physical properties compared with those in bulk materials[7] and they have great potential technological applications in various areas; for example, they can be used in biomedical applications,[8,9] sensors,[10] nonlinear optics,[11] permanent magnets,[12] environmental remediation,[13] and information storage devices.[14–16]

Theoretically, the magnetic properties of nanomaterials have been studied by various techniques, such as variational cumulant expansion (VCE),[17,18] Green functions (GF) formalism,[19] mean-field theory (MFT),[20–26] effective field theory (EFT) with correlations,[23–42] and Monte Carlo (MC) simulations.[43–58] From these studies we can see that the core-shell structure can be successfully performed to nanomagnetism for nanomaterials. Hence, the aforementioned techniques are capable of explaining diverse typical behaviors found in nanomagnetism. In order to simulate the behaviors of many complex systems, such as magnetic nanoparticle systems, the MC simulation[59] is a strong numerical approach. However, this method has a disadvantage in that the long calculation times originating from the exhausting sampling averaging procedures require large computer resources. On the other hand, due to its mathematical simplicity, the EFT is considered to be superior to conventional MFT since it partially considers the spin–spin correlations and, as a result, it gives more accurate results than the MFT in the calculations. Kaneyoshi[23] was the first to introduce the EFT formalism for ferroelectric nanoparticles. In a series of the sequential studies, he extended the theory for the investigation of thermal and magnetic properties of the nanoscaled transverse Ising thin films,[26] and also for cylindrical nanowire and nanotube systems.[24,25,27–29]

Despite these studies, as far as we know, the thermal and magnetic properties of a spin-1/2 hexagonal Ising nanowire (HIN) have not been investigated. Therefore, in this paper, the effects of the core/shell exchange interfacial coupling and the exchange interaction coupling in the surface, on the thermal and magnetic properties of HIN system with core/shell structure are discussed within the framework of the EFT with correlations.

This paper is organized as follows. In Section 2, the model and formalism of the EFT with correlation is presented briefly. The detailed numerical result and discussion are given in Section 3. Finally, Section 4 is devoted to a summary and a brief conclusion.

2. Model and formulation

The schematic representation of a hexagonal Ising nanowire (HIN) system with core/shell structure is shown in Fig. 1. The blue and red spheres indicate magnetic atoms at the surface shell and core, respectively. Each site of the HIN system is occupied by a spin-1/2 magnetic atoms and each magnetic atom is connected to the two nearest-neighbor magnetic atoms on the above and below sections along the wire. The Hamiltonian of the system is given by

$$H = -J_{\mathrm{S}}\sum_{\langle ij\rangle} S_i S_j - J_{\mathrm{C}}\sum_{\langle mn\rangle} S_m S_n - J_1\sum_{\langle im\rangle} S_i S_m - h\Big(\sum_i S_i + \sum_m S_m\Big), \quad (1)$$

where $\langle ij\rangle$, $\langle mn\rangle$, and $\langle im\rangle$ denote the summations over all pairs of neighboring spins at the shell surface, core and be-

†Corresponding author. E-mail: ersinkantar@erciyes.edu.tr

© 2014 Chinese Physical Society and IOP Publishing Ltd

tween shell surface and core, respectively. S_i are the Pauli spin operator and h is the external magnetic field. The J_S and J_C are the interaction parameters between two nearest-neighbor magnetic atoms at the surface shell and core, respectively, and J_1 is the interaction parameter between two nearest-neighbor magnetic atoms at the surface shell and the core. In order to clear up of the surface effects on the physical properties of the system, the J_S surface interaction parameter is often defined as $J_S = J_C(1+\Delta_S)$.[25,29,32,34] According to the framework of EFT, we can easily obtain m_C magnetization at the core and m_S magnetization in the shell surface for the HIN system depicted in Fig. 1, as follows:

$$m_C = [\cosh(J_C\nabla) + m_C \sinh(J_C\nabla)]^2 \times [\cosh(J_1\nabla) + m_S \sinh(J_1\nabla)]^6 F_C(x+h)|_{x=0}, \quad (2a)$$

$$m_S = [\cosh(J_S\nabla) + m_S \sinh(J_S\nabla)]^4 \times [\cosh(J_1\nabla) + m_C \sinh(J_1\nabla)]F_S(x+h)|_{x=0}, \quad (2b)$$

where $\nabla = \partial/\partial x$ is the differential operator. The $F_C(x+h)$ and $F_S(x+h)$ functions are defined as follows:

$$F_C(x+h) = F_S(x+h) = \tanh[\beta(x+h)]. \quad (3)$$

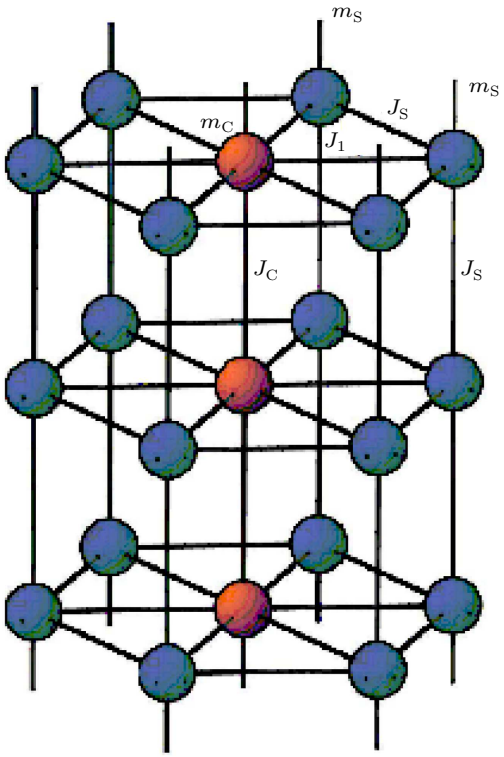


Fig. 1. (color online) The schematic representation of a hexagonal Ising nanowire. The blue and red spheres indicate magnetic atoms at the surface shell and core, respectively.

In Eq. (3), $\beta = 1/k_B T$ where k_B is the Boltzmann constant and T is temperature. By expanding the right-hand side of Eq. (2), we can obtain two coupled nonlinear equations. By solving the equations numerically we can get m_C and m_S magnetizations. The total magnetization per site can be obtained via $m_T = 1/7(m_C + 6m_S)$. For the following discussions, at this point let us define the r parameter as $r = J_1/J_C$. If the value of r is selected as $r > 0$ (positive core–shell interfacial coupling), then the spin directions at the shell surface and core are parallel and thus the spin-configuration of the system may show ferromagnetic behavior. If the value of r is selected as $r < 0$ (negative core–shell interfacial coupling), then the spins at the shell surface are directed opposite to those in the core and, hence, the system exhibits a ferrimagnetic spin-configuration, as discussed in Refs. [27]–[29].

In order to obtained susceptibilities of the system, we differentiated magnetizations with respect to h, as in the following equation:

$$\chi_\alpha = \lim_{\to 0}\left(\frac{\partial m_\alpha}{\partial h}\right), \quad (4)$$

where, $\alpha =$ C and S. By using Eqs. (2) and (4), we can easily obtain the χ_C and χ_S susceptibilites as follows:

$$\chi_C = a_1\chi_C + a_2\chi_S + a_3\frac{\partial F_C(x)}{\partial h}, \quad (5a)$$

$$\chi_S = b_1\chi_S + b_2\chi_C + b_3\frac{\partial F_S(x)}{\partial h}. \quad (5b)$$

Here, a_i and b_i ($i = 1$, 2, and 3) coefficients have complicated and long expressions and, hence, they will not given. The total susceptibilities per site can be obtained via $\chi_T = 1/7(\chi_C + 6\chi_S)$.

The internal energy of per site of the system can be calculated as

$$\frac{U}{N} = -\frac{1}{2}(\langle U_C\rangle + \langle U_S\rangle) - h(\langle m_C\rangle + \langle m_S\rangle), \quad (6)$$

where,

$$\langle U_C\rangle = \frac{\partial}{\partial\nabla}[\cosh(J_C\nabla) + m_C \sinh(J_C\nabla)]^2 \times [\cosh(J_1\nabla) + m_S \sinh(J_1\nabla)]^6 F_C(x+h)|_{x=0}, \quad (7a)$$

$$\langle U_S\rangle = \frac{\partial}{\partial\nabla}[\cosh(J_S\nabla) + m_S \sinh(J_S\nabla)]^4 \times [\cosh(J_1\nabla) + m_C \sinh(J_1\nabla)]F_S(x+h)|_{x=0}. \quad (7b)$$

The specific heat of the system can be obtained from the relation

$$C_h = \left(\frac{\partial U}{\partial T}\right)_h. \quad (8)$$

The Helmholtz free energy of the system can be defined as

$$F = U - TS, \quad (9)$$

in which, according to the third law of thermodynamics, it can be written in the form

$$F = U - T\int_0^T \frac{C}{T'}\,\mathrm{d}T'. \quad (10)$$

The second term on the right-hand side of Eq. (10) (the integral which appears) is the entropy of the system according to the second law of the thermodynamics.

3. Numerical results and discussion

In this section, we investigate some interesting and typical results of the HIN system with core/shell structure. Some thermodynamic and magnetic quantities (magnetization, susceptibility, internal energy, specific heat, and free energy) and hysteresis curves of the HIN system with core/shell structure

are studied and discussed for selected values of the interaction parameters. Moreover, the behavior of the total magnetization as a function of the temperature will be investigated to find the types of compensation behavior of the system.

3.1. Thermal and magnetic behaviors

We examine the thermal and magnetic behavior of total magnetization, susceptibility, internal energy, specific heat, and free energy of the system. Firstly, we have fixed $J_C = 1.0$ and $k_B = 1.0$ throughout the paper. A few explanatory and interesting results are plotted in Figs. 2 and 3 for ferromagnetic and antiferromagnetic interactions, respectively. It has been found that the system shows second-order phase transition. In order to confirm that we find correct phase transitions, we also investigate the free energy of the system. Figure 2 illustrates the thermal variation of the m_T (total magnetization), χ_T (total susceptibility), U_T (total internal energy), C (specific heat), and F (free energy) for ferromagnetic interface coupling $r > 0$, and r changes from 0.01 to 1.0, and $\Delta_S = 0.0$. In Fig. 2(a),

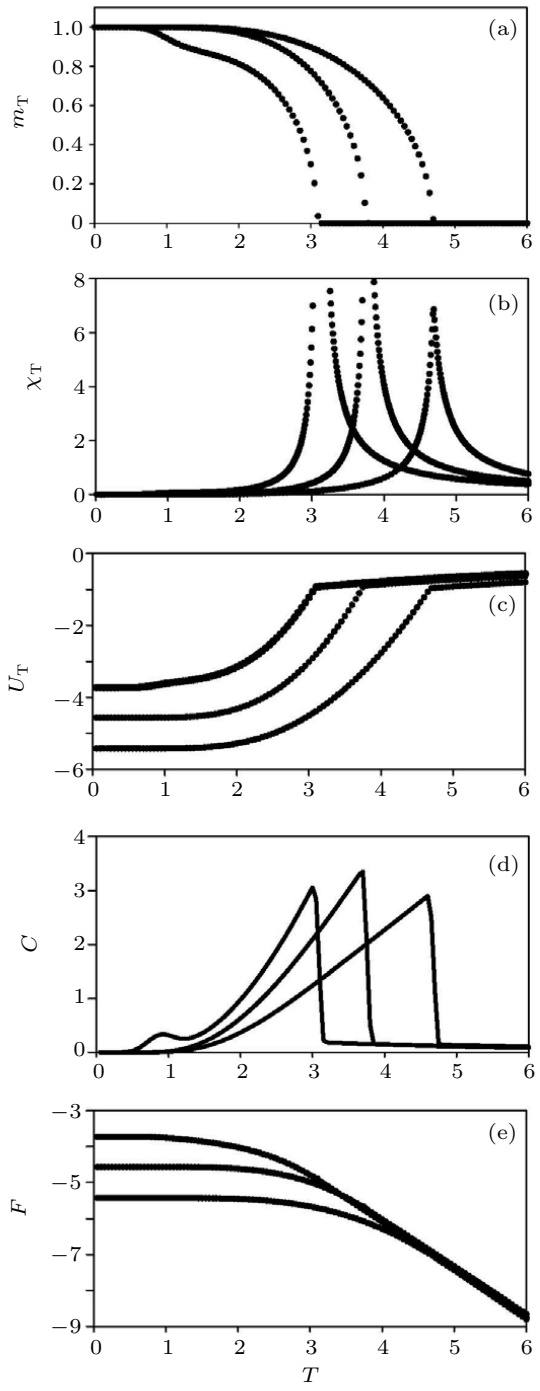


Fig. 2. Thermal variations of the magnetizations (m), susceptibilities (χ), internal energy (U), and free energy (F) with various values of r, Δ_S, and D for the ferromagnetic interface coupling ($r > 0$).

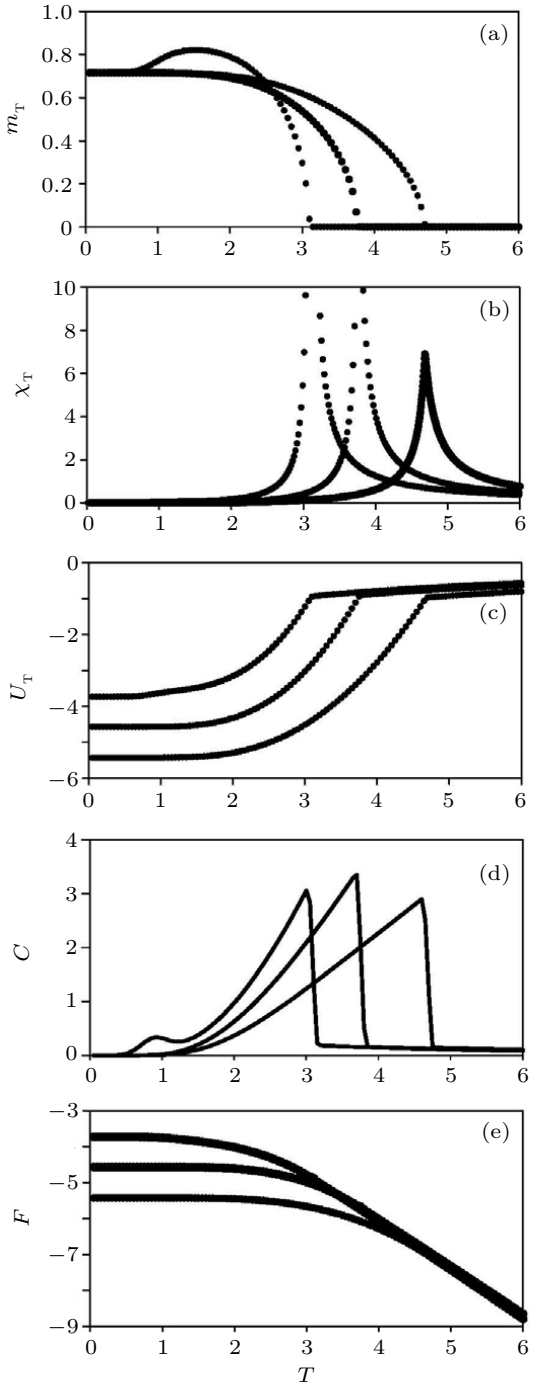


Fig. 3. Thermal variations of the magnetizations (m), susceptibilities (χ), internal energy (U), and free energy (F) with various values of r, Δ_S, and D for the antiferromagnetic interface coupling ($r < 0$).

the total magnetizations decrease to zero continuously as the temperature increases; therefore, a second-order phase transition occurs. When the temperature approaches T_C, the susceptibilities χ_T increase very rapidly and go to infinity at T_C, as seen in Fig. 2(b). Figure 2(c) illustrates the behavior of the internal energies. It expresses a discontinuity of the curvature at the critical temperature T_C. The specific heat curves of the HIN system exhibit second-order phase transition at T_C and rapidly decrease with the increasing temperature, as seen in Fig. 2(d). On the other hand, figure 3 shows the temperature dependence of m_T, χ_T, U_T, C, and F for antiferromagnetic interface coupling $r < 0$, and r changes from -0.01 to -1.0, and $\Delta_S = 0.0$. In Fig. 3(a), the total magnetizations decrease continuously with increasing values of temperature, and they become zero at T_C; therefore, a second-order phase transition occurs. In Figs. 3(b) and 3(c), the temperature dependence of susceptibilities and internal energies are depicted, respectively. In these figures, the susceptibilities increase very rapidly and go to infinity at T_C, and the internal energies make a cusp at T_C.

3.2. Compensation behavior

We studied the compensation behaviors of the HIN system, in which we know that a compensation temperature can be found in the nanostructure systems.[27,37] Figure 4 shows the temperature dependencies of the total magnetization

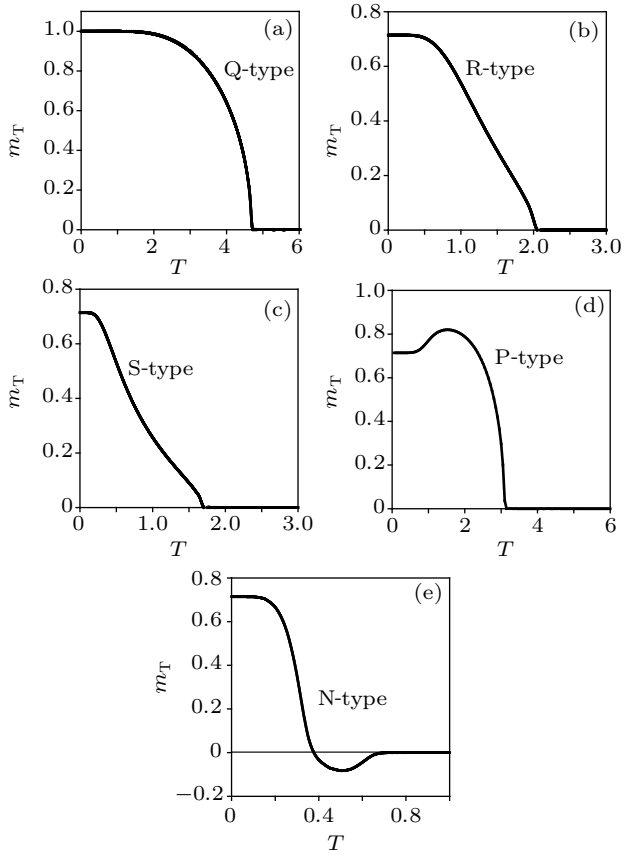


Fig. 4. The total magnetization as a function of the temperature for different values of interaction parameters. The system exhibits the Q-, R-, N-, P-, and S-types of compensation behaviors. (a) $r = 1.0$ and $\Delta_S = 0.0$, (b) $r = -0.5$ and $\Delta_S = -0.8$, (c) $r = -0.5$ and $\Delta_S = -0.99$, (d) $r = -0.01$ and $\Delta_S = 0.0$, (e) $r = -0.01$ and $\Delta_S = -0.9$.

m_T for several values of r and Δ_S. As seen from Fig. 4(a), the curve labeled $r = 1.0$ and $\Delta_S = 0.0$ may show the Q-type behavior. The R-type behavior is obtained in Fig. 4(b) for $r = -0.5$ and $\Delta_S = -0.8$. Figure 4(c) is calculated for $r = -0.5$ and $\Delta_S = -0.99$. As we can see, this curve illustrates the S-type behavior. Figure 3(d) is calculated for $r = -0.1$ and $\Delta_S = 0$, and illustrates the P-type behavior. Moreover, the N-type behavior is presented in Fig. 4(e) for $r = -0.1$ and $\Delta_S = -0.9$. These obtained results are consistent with same behavior as that classified in the Neél theory.[60,61]

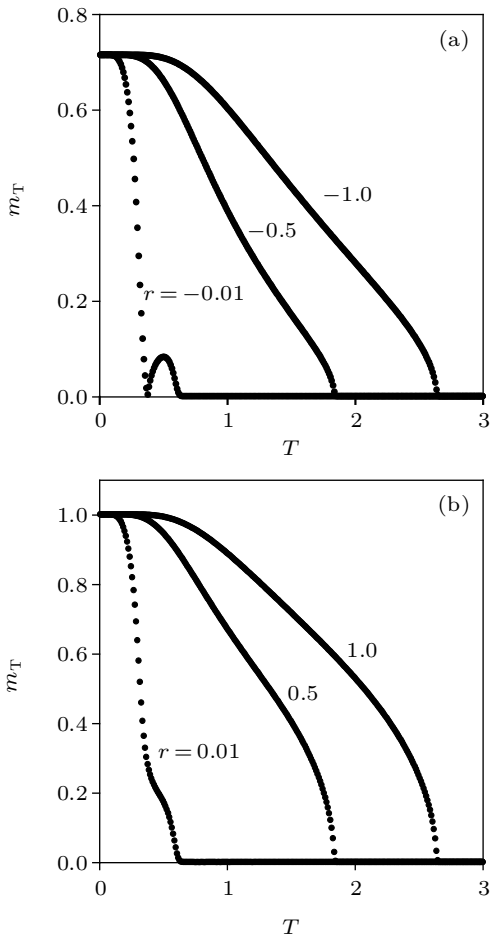


Fig. 5. The effect of the ferromagnetic and antiferromagnetic interface coupling between the shell and core spins on the thermal properties of the total magnetization for some selected values of $r = J_1/J_C$ with $\Delta_S = -0.9$.

On the other hand, in order to clarify the effect of the ferromagnetic and antiferromagnetic interface coupling between the shell surface and core spins on the thermal properties of the total magnetization, two representative and interesting results are presented in Fig. 5. Figure 5 is obtained for some selected values of r and Δ_S. Figure 5(a) shows the temperature dependences of the total magnetization for the antiferromagnetic interface coupling $r < 0$, and r changes from -0.01 to -1.0. The curves labeled $r = -0.01$ exhibits the N-type behavior. As seen from the figure, the S-type behavior is obtained for $r = -0.5$, and the R-type behavior is obtained for $r = -1.0$. In Fig. 5(b), we illustrate the thermal behavior of the total magnetization for the ferromagnetic interface coupling $r > 0$, and

r changes from 0.01 to 1.0. The curve labeled $r = 0.01$ shows the S-type behavior. As seen from the figure, the R-type and Q-type behaviors are observed for $r = 0.5$ and $r = 1.0$, respectively. As a final remark, it can be also seen from Figs. 5(a) and 5(b) that changing the sign of the interface coupling r does not affect the critical temperature. We also examine the effects of the surface coupling between the shell surface spins on the compensation behaviors in the system. In Figs. 6(a) and 6(b), we illustrate the total magnetization versus reduced temperature for the ferromagnetic and antiferromagnetic interface couplings $r = 1.0$ and $r = -1.0$, respectively, changing the value of Δ_S from $\Delta_S = 0.0$ to -0.9. In Fig. 6(a), the curve labeled $\Delta_S = -0.5$ and 0.0 exhibits the Q-type behavior. As can also seen from the figure, the R-type behavior is obtained for $\Delta_S = -0.9$. In Fig. 6(b), the curve labeled $\Delta_S = 0.0, -0.5$, and -0.9 shows the Q-type behavior.

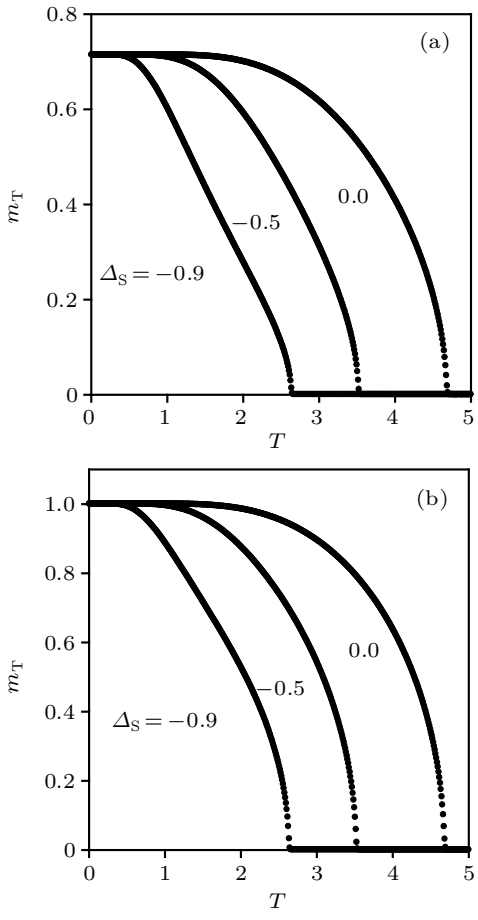


Fig. 6. The effects of the surface coupling between the shell spins on the total magnetization with $r = 1.0$ and -1.0, changing the value of Δ_S from $\Delta_S = 0.0$ to -0.9. (a) For ferromagnetic case and $\Delta_S = 0.0, -0.5$, and -0.9; (b) for antiferromagnetic case and $\Delta_S = 0.0, -0.5$, and -0.9.

3.3. Hysteresis behavior

3.3.1. The influence of the temperature

In order to investigate the influence of the temperature on the hysteresis behaviors of the HIN system in the case of $r = 0.01$, a series of hysteresis loops for two regimes $T < T_C$ ($T = 0.5$, 1.0, 1.5, and 2.0) and $T > T_C$ ($T = 3.5$) are plotted in Fig. 7 with fixed parameter, $\Delta_S = 0.0$. From Figs. 7(a)–7(c) $T < T_C$, we can see that we have a double loops ferromagnetic hysteresis loop. The single hysteresis loop appears when the temperature approaches its critical value $T_C = 3.2$, as seen in Fig. 7(d). If the temperature grows stronger, then the single hysteresis loop disappears in the case of $T > T_C$, as seen in Fig. 7(e). Moreover, the hysteresis loops decrease as the temperature increases. These results are consistent with some experimental[62–67] and theoretical results.[54,56,68,69]

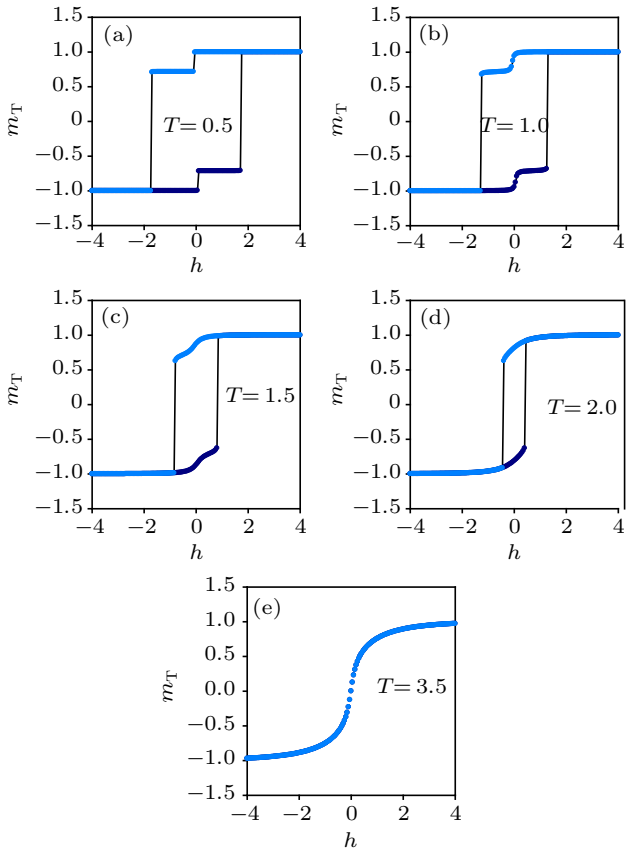


Fig. 7. (color online) The effects of the temperature field on the hysteresis behavior for $r = 0.01$, $\Delta_S = 0.0$, and $T = 0.5$, 1.0, 1.5, 2.0 and 3.5.

3.3.2. The influence of the ferromagnetic and antiferromagnetic interfacial couplings

Our investigations in this work are for both ferromagnetic and antiferromagnetic cases. Hence, $J_1 > 0$ (positive core–shell coupling) and $J_1 < 0$ (negative core–shell coupling) correspond to the ferromagnetic and antiferromagnetic interfacial couplings, respectively. In Fig. 8, we show the dependence of the hysteresis loops of the HIN system on the ferromagnetic interface coupling constant ($r = 1.0$, 0.25, and 0.01) at $T = 0.5$ for $\Delta_S = 0.0$. We can see that if the antiferromagnetic coupling constant is small (Fig. 8(a)), only a central loop opens. It is shown that when r increases (Fig. 8(b)) the hysteresis curve changes from one central loop to triple loops, and then the triple loops turn to a double central loop. In Fig. 9, we show the dependence of the hysteresis loops of the HIN system on the interfacial couplings ($r = -1.0$, -0.5, and -0.01)

at $T = 0.5$ for $\Delta_S = 0.0$. As the interfacial coupling decreases, the single central loop turns to a double loop.

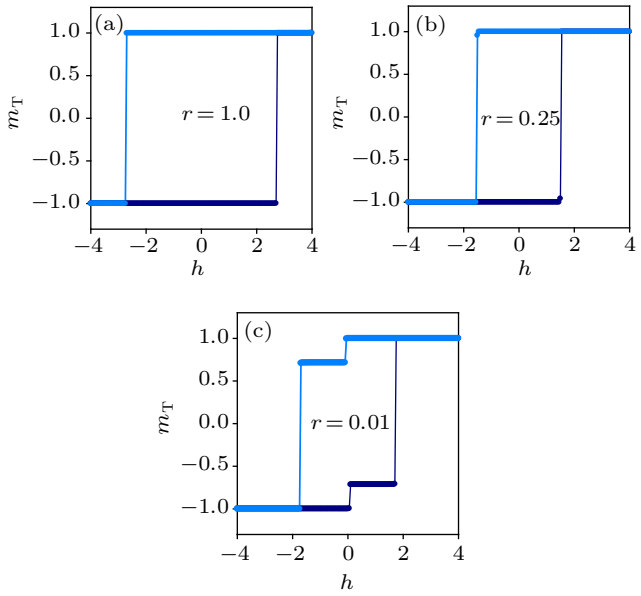


Fig. 8. (color online) The effect of the ferromagnetic interface coupling between the shell and core spins on the hysteresis behavior for $T = 0.5$, $\Delta_S = 0.0$, and $r = 1.0$, 0.25, and 0.01.

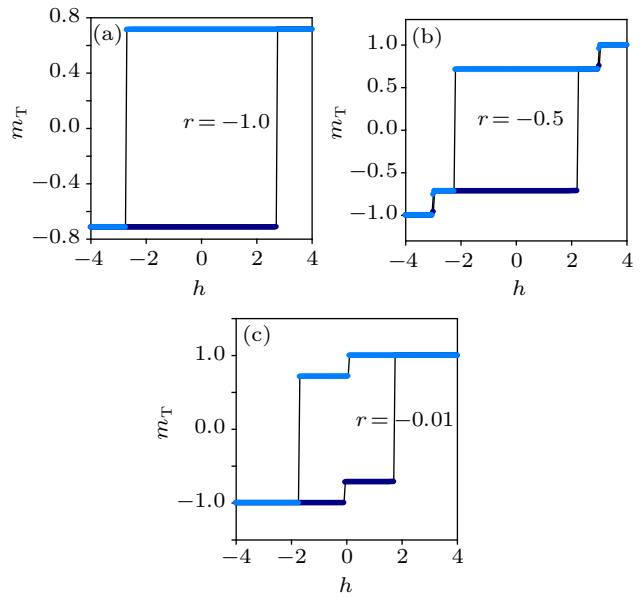


Fig. 9. (color online) The effect of the antiferromagnetic interface coupling between the shell and core spins field on the hysteresis behavior for $T = 0.5$, $\Delta_S = 0.0$, and $r = -1.0$, -0.5, and -0.01.

4. Summary and conclusion

In this paper, we have studied the thermal magnetic properties (magnetizations, susceptibilities, internal energies, free energies, hysteresis curves, and compensation behaviors) of spin-1/2 HIN system by using the effective-field theory with correlations. We investigated the thermal variations of total magnetizations, as seen in Figs. 2(a) and 3(a). It has been shown that the system only undergoes a second-order phase transition. Moreover, from the thermal variations of the total magnetization, the five compensation types can be found under certain conditions, namely the Q-, R-, S-, P-, and N-types. We should also mention that when the MFT is applied to the present system, for example, the behaviors of susceptibility and specific heat in Figs. 2 and 3 may exhibit a shoulder or a divergence below its transition temperature, with decreasing values of r, like Figs. 2 and 3. These facts are sharply in contrast to the results of Figs. 2 and 3, which are completely artifacts of the MFT. The reason comes from the fact that the MFT gives two finite transition temperatures when $r = 0.0$. Finally, we hope that the study of the HIN system may open a new ferrimagnetism as well as new field in the research of magnetism and the present work will be potentially helpful for studying higher spins and more complicated nanowire systems.

References

[1] Skumryev V, Stoyanov, Zhang Y, Hadjipanayis G C, Givord D and Nogués J 2003 *Nature* **423** 850
[2] Zhong Z, Wang D, Cui Y, Bockrath M W and Lieber C M 2003 *Science* **302** 1377
[3] Liu Z, Zhang D, Han S, Li C, Lei B, Lu W, Fang J and Zhou C 2005 *J. Am. Chem. Soc.* **127** 6
[4] Skomski R 2003 *J. Phys.: Condens. Matter* **15** 841
[5] Denisov S I, Lyutyy T V, Hanggi P and Trohidou K N 2006 *Phys. Rev. B* **74** 104406
[6] Zou X and Xiao G 2008 *Phys. Rev. B* **77** 054417
[7] Berkowitz A E, Kodama R H, Makhlouf S A, Parker F T, Spada F E, McNiff E J and Foner S 1999 *J. Magn. Magn. Mater.* **196** 591
[8] Alexiou C, Schmidt A, Klein R, Hullin P, Bergemann C and Arnold W 2002 *J. Magn. Magn. Mater.* **252** 363
[9] Sounderya N and Zhang Y 2008 *Rec. Pat. Biomed. Engin.* **1** 34
[10] Kurlyandskaya G V, Sanchez M L, Hernando B, Prida V M, Gorria P and Tejedor M 2003 *Appl. Phys. Lett.* **82** 3053
[11] Nie S and Emory S R 1997 *Science* **275** 1102
[12] Zeng H, Li J, Liu J P, Wang Z L and Sun S 2002 *Nature* **420** 395
[13] Elliott D W and Zhang W X 2001 *Environ. Sci. Tech.* **35** 4922
[14] Wegrowe J E, Kelly D, Jaccard Y, Guittienne Ph and Ansermet J Ph 1999 *Europhys. Lett.* **45** 626
[15] Fert A and Piraux L 1999 *J. Magn. Magn. Mater.* **200** 338
[16] Kodama R H 1999 *J. Magn. Magn. Mater.* **200** 359
[17] Wang H, Zhou Y, Wang E and Lin D L 2001 *Chin. J. Phys.* **39** 85
[18] Wang H, Zhou Y, Lin D L and Wang C 2002 *Phys. Status Solidi B* **232** 254
[19] Garanin D A and Kachkachi H 2003 *Phys. Rev. Lett.* **90** 65504
[20] Leite V S and Figueiredo W 2005 *Physica A* **350** 379
[21] Kaneyoshi T 2009 *Phys. Status Solidi B* **246** 2359
[22] Kaneyoshi T 2009 *J. Magn. Magn. Mater.* **321** 3430
[23] Kaneyoshi T 2005 *Phys. Status Solidi B* **242** 2938
[24] Kaneyoshi T 2010 *J. Magn. Magn. Mater.* **322** 3014
[25] Kaneyoshi T 2011 *J. Magn. Magn. Mater.* **323** 1145
[26] Kaneyoshi T 2012 *Phase Transit.* **85** 264
[27] Kaneyoshi T 2011 *Physica A* **390** 3697
[28] Kaneyoshi T 2011 *Solid State Commun.* **151** 1528
[29] Kaneyoshi T 2011 *Phys. Status Solidi B* **248** 250
[30] Canko O, Erdinc A, Taskın F and Atis M 2011 *Phys. Lett. A* **375** 3547
[31] Wang C D, Lu Z Z, Yuan W X, Kwok S Y and Teng B H 2011 *Phys. Lett. A* **375** 3405
[32] Keskin M, Şarlı N and Deviren B 2011 *Solid State Commun.* **151** 1025
[33] Kaneyoshi T 2012 *Physica A* **391** 3616
[34] Şarlı N 2013 *Physica B* **411** 12
[35] Canko O, Erdinc A, Taskın F and Yıldırım A F 2012 *J. Magn. Magn. Mater.* **324** 508
[36] Jiang W, Guan H, Wang Z and Guo A 2012 *Physica B* **407** 378
[37] Kaneyoshi T 2012 *Solid State Commun.* **152** 883
[38] Bouhou S, Essaoudi I, Ainane A, Saber M, Dujardin F and de Miguel J J 2012 *J. Magn. Magn. Mater.* **324** 2434
[39] Liu L M, Jiang W, Wang Z, Guan H Y and Guo A B 2012 *J. Magn. Magn. Mater.* **324** 4034

[40] Jiang W, Guan H Y, Wang Z and Guo A B 2012 *Physica B* **407** 378
[41] Jiang W, Zhang F, Li X X, Guan H Y, Guo A B and Wang Z 2013 *Physica E* **47** 95
[42] Jiang W, Li X X and Liu L M 2013 *Physica E* **53** 29
[43] Eftaxias E and Trohidou K N 2005 *Phys. Rev. B* **71** 134406
[44] Iglesias O, Batlle X and Labarta A 2005 *Phys. Rev. B* **72** 212401
[45] Kechrakos D, Trohidou K N and Vasilakaki M 2007 *J. Magn. Magn. Mater.* **316** e291
[46] Hu Y and Du A 2007 *J. Appl. Phys.* **102** 113911
[47] Trohidou K N, Vasilakaki M, Bianco L Del, Fiorani D and Testa A M 2007 *J. Magn. Magn. Mater.* **316** e82
[48] Wu M H, Li Q C and Liu J M 2007 *J. Phys.: Condens. Matter* **19** 186202
[49] Iglesias O, Batlle X and Labarta A 2007 *J. Phys.: Condens. Matter* **19** 406232
[50] Iglesias O, Batlle X and Labarta A 2008 *J. Nanosci. Nanotechnol.* **8** 2761
[51] Vasilakaki M, Eftaxias E and Trohidou K N 2008 *Phys. Status Solidi A* **205** 1865
[52] Vasilakaki M and Trohidou K N 2009 *Phys. Rev. B* **79** 144402
[53] Hu Y and Du A 2009 *Phys. Status Solidi B* **246** 2384
[54] Hu Y, Liu L and Du A 2010 *Phys. Status Solidi B* **247** 972
[55] Zaim A, Kerouad M and Amraoui Y El 2009 *J. Magn. Magn. Mater.* **321** 1083
[56] Zaim A and Kerouad M 2010 *Physica A* **389** 3435
[57] Jiang L, Zhang J, Chen Z, Feng Q and Huang Z 2010 *Physica B* **405** 420
[58] Yüksel Y, Aydıner E and Polat H 2011 *J. Magn. Magn. Mater.* **323** 3168
[59] Metropolis N, Rosenbluth A W, Rosenbluth M N, Teller A H and Teller E 1953 *J. Chem. Phys.* **21** 1087
[60] Neél L 1948 *Annals of Physics* (Amsterdam: Netherlands) **3** 137
[61] Chikazumi S 1997 *Physics of Ferromagnetism* (Oxford: Oxford University Press)
[62] Zhou H, Yiu Y, Aronson M C and Wong S S 2008 *J. Solid State Chem.* **181** 1539
[63] Duan J, Liu J, Cornelius T W, Yao H, Mo D, Chen Y, Zhang L, Sun Y, Hou M, Trautmann C and Neumann R 2009 *Nucl. Instrum. Methods Phys. Res. B* **267** 2567
[64] Fleaca C T, Morjan I, Alexandrescu R, Dumitrache F, Soare I, Gavrila-Florescu L, Normand F Le and Derory A 2009 *Appl. Surf. Sci.* **255** 5386
[65] Lupu N, Lostun L and Chiriac H 2010 *J. Appl. Phys.* **107** 09E315
[66] Wu H W, Tsai C J and Chen L J 2007 *Appl. Phys. Lett.* **90** 043121
[67] Curiale J, Sanchez R D, Troiani H E, Leyva A G and Levy P 2005 *Appl. Phys. Lett.* **87** 043113
[68] Zaim A, Kerouad M and Amraoui Y El 2009 *J. Magn. Magn. Mater.* **321** 1077
[69] Chong Y T, Gorlitz D, Martens S, Yau M Y E, Allende S, Bachmann J and Nielsch K 2010 *Adv. Mater.* **22** 2435